Monte Carlo Simulations of Partially Ionized Polyelectrolytes: Conformational Properties

George A. Christos*

School of Mathematics and Statistics, GPO Box U1987, Curtin University of Technology, Perth, 6001 Australia

Steven L. Carnie

Department of Mathematics, University of Melbourne, Parkville, 3052 Australia

Trevor P. Creamer

Department of Biochemistry and Biophysics, University of North Carolina, Chapel Hill, North Carolina 27514-7231

Received June 17, 1991; Revised Manuscript Received September 17, 1991

ABSTRACT: We present results of Monte Carlo simulations of partially ionized polyelectrolytes where the charged beads interact through screened Coulomb potentials of Debye–Hückel form. We discuss the behavior of the mean square end-to-end distance versus chain length for a variety of degrees of ionization and added salt concentrations, including the dependence of the apparent scaling exponent on the degree of ionization. We also present estimates for the infinite-chain persistence length, obtained both directly from finite-chain results and by extrapolation from the distribution of bond angles relative to the central bond.

1. Introduction

In this paper we extend our previous work on the conformational properties of isolated polyelectrolyte chains with screened Coulomb interactions between charged beads[1] to the case of partially ionized chains. In terms of the models described in ref 1, all the results here are for the free-rotation model—that is, the chains have fixed bond length (l) and bond angle (θ) but no torsional potential. As in ref 1, model parameters (bond length and bead size) have been chosen to correspond roughly to those of polyacrylic acid (PAA) but where each bead represents a repeat unit.

This model was chosen partly because it showed a lower rate of rejection of Monte Carlo moves and lower serial correlation between blocks of moves. In addition, the hindered rotation model of ref 1 showed large oscillations in the distribution of angles of bonds relative to the central bond. These oscillations arise from the combination of the torsional potential with our location of the charges at the center of each bead (since each bead represents a repeat unit). Calculations on a more realistic model for PAA which models the (uncharged) carbon backbone and (charged) side groups explicitly[2] gave results much closer to the free-rotation model (with repeat-unit beads) than to the hindered-rotation model. Of course, there are synthetic polyelectrolytes which have charged backbone groups [poly(ethylene imine), for example], but they typically have a lower linear charge density than the chains studied in ref 1.

The details of the simulation method for partially ionized chains have been described elsewhere[3]—we use the same procedure here except that the statistical averages are calculated from every configuration, rather than just one configuration per block. This procedure results in somewhat less (statistically) variable results than those presented in ref 3.

It is pertinent at this stage to comment on our use of the term "partially ionized". We have performed simulations on chains with the fraction of beads being charged ranging from 100% (which we have called "fully ionized") to 10%. We have called this fraction the degree of ionization, α. However, we are not particularly focused on weak polyelectrolytes but use α to vary the linear charge density on the chain, whether that comes about from partially neutralizing a weak polyacid (admittedly a common case) or from the method of synthesis [see, for example, the way linear charge density is varied in poly(acrylic acid/acrylamide) copolymers[4] or the tailoring of a desired linear charge density by synthesizing an appropriate poly(imine)[5]]. By setting the linear charge density and the salt concentration as independent variables, we are concentrating on the physical interactions causing the conformation of the chain, rather than the mechanism by which the chain has become charged. This procedure is very commonly followed in theoretical discussions of general polyelectrolyte behavior, such as rod models[6] or wormlike chain models.[7] In summary, we study the behavior of a chain for a given value of α and salt concentration (c), however, that came about. Instead of "partially ionized", we could have used the term "with various linear charge densities".

In statistical mechanical terms, we have performed the simulations in the constant surface charge ensemble, rather than the constant surface chemical potential ensemble (in which the linear charge density would be a fluctuating quantity).

If one is primarily interested in weak polyacids and wants to generate theoretical titration curves, as in ref 8, then one has to model the particular dissociation reaction and use c and pH as independent variables for a given pK. This is certainly of interest but not what we are pursuing in this paper.

2. Results

We present results for the mean-square end-to-end distance, $\langle r^2 \rangle$, the persistence length, L_p, and the distribution of angles of bonds relative to the central bond, $\langle \cos \psi_k \rangle$. Trends for the mean-square radius of gyration, $\langle s^2 \rangle$, are very similar to those for $\langle r^2 \rangle$, and results for $\langle s^2 \rangle$ can also be found in ref 3. For ion concentration $c = 10^{-1}$ mol dm^{-3}, we calculated these properties for chain lengths N = 20, 40, 80, 120, 160, 200, 240, and 320 and for degrees

0024-9297/92/2225-1121$03.00/0

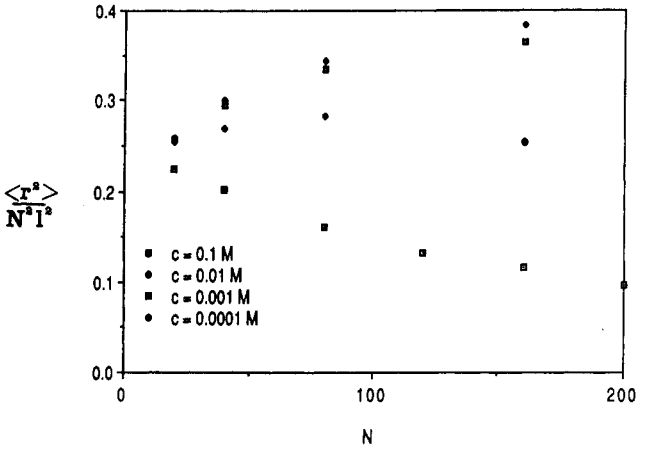

Figure 1. Mean-square end-to-end distance of the polyion chains (plotted as $\langle r^2\rangle/N^2l^2$) for degree of ionization $\alpha = 0.5$ and various added salt concentrations.

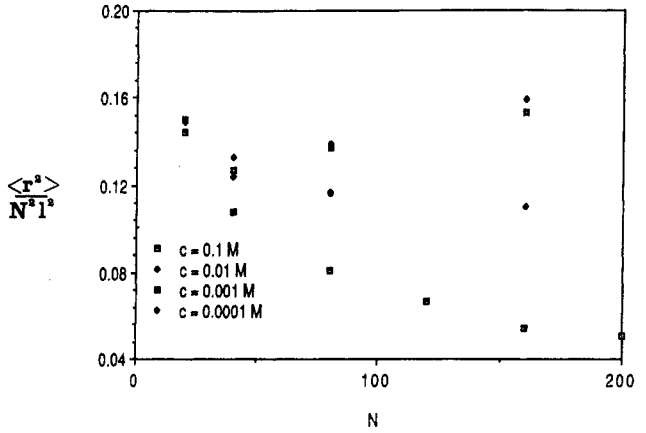

Figure 2. As for Figure 1, but for $\alpha = 0.2$.

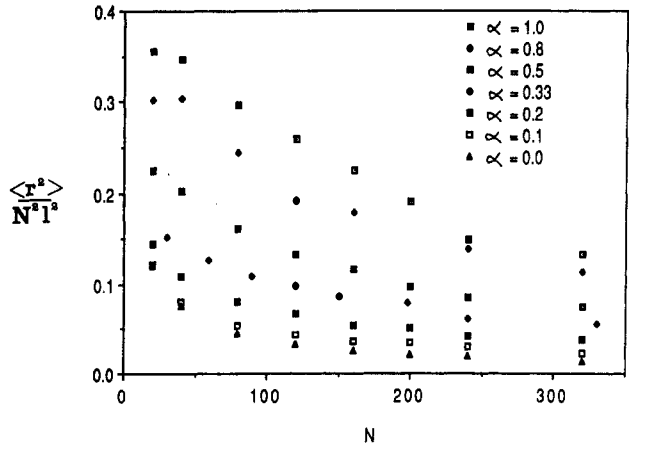

Figure 3. Mean-square end-to-end distance for salt concentration $c = 0.1$ mol dm^{-3} and various degrees of ionization.

of ionization $\alpha = 0$, 0.1, 0.2, 0.5, 0.8, and 1.0. For $\alpha = {}^1/_3$, the chain lengths used were $N = 30$, 60, 90, 120, 150, 198, 240, and 330. At lower ion concentrations ($c = 10^{-2}$, 10^{-3}, 10^{-4} mol dm^{-3}), calculations were done for chain lengths $N = 20$, 40, 80, and 160 and degrees of ionization $\alpha = 0$, 0.1, 0.2, 0.5, 0.8, and 1.0. For $\alpha = {}^1/_3$, the chain lengths were $N = 30$, 60, 90, and 150. Results for the fully ionized case ($\alpha = 1.0$) have been discussed in ref 1 and will not be presented here. In each case, the number of configurations was $\approx 100\,N^2$—usually sufficient to ensure statistical errors of around 2%.

In Figures 1–4 we plot $\langle r^2\rangle/N^2l^2$ as a function of chain length for various concentrations and degrees of ionization.

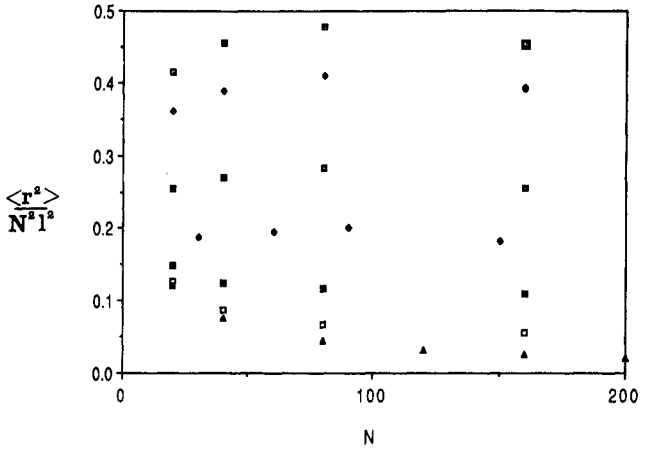

Figure 4. As for Figure 3, but for $c = 0.01$ mol dm^{-3}: $\alpha = 1.0$ (▣), 0.8 (♦), 0.5 (□), 0.33 (◇), 0.2 (■), 0.1 (□), 0.0 (▲).

On such a plot, Gaussian coil behavior ($\langle r^2\rangle \approx N$) is reflected in an N^{-1} dependence on chain length, and rigid rod behavior ($\langle r^2\rangle \approx N^2$) corresponds to horizontal lines. Polyelectrolytes can show behavior intermediate between these extremes.

Results for the mean-square end-to-end distance for $\alpha = 0.5$ and $c = 10^{-1}$, 10^{-2}, 10^{-3}, and 10^{-4} mol dm^{-3} are shown in Figure 1. The behavior is rather similar to that seen in fully ionized chains,[1] except that the values are somewhat smaller, as expected. At $c = 0.1$ mol dm^{-3}, the values continually decrease, indicating coil-like behavior. For lower concentrations, the initial increase with N is due to the fact that the contour length is smaller than a few screening lengths ($\kappa^{-1} \propto c^{-1/2}$). Once the chain gets sufficiently long, $\langle r^2\rangle/N^2$ again starts to fall.

In Figure 2 we show results for the same concentrations but for degree of ionization $\alpha = 0.2$. Overall the values have again decreased as expected, but all the curves show an initial decrease with N. We interpret this as due to the small number of charges on the chain at low values of α and N—the chain behaves almost as if it were uncharged. For low ion concentrations (i.e. large screening lengths), as the number of charges on the chain gets large enough for electrostatic effects to be significant, $\langle r^2\rangle/N^2$ again rises with N until the contour length approaches a few screening lengths. Although we have no data for longer chains, we would expect $\langle r^2\rangle/N^2$ to decrease with N thereafter, even at low ion concentrations.

A plot of $\langle r^2\rangle/N^2l^2$ versus chain length at $c = 0.1$ mol dm^{-3} and degrees of ionization $\alpha = 0$, 0.1, 0.2, 0.333, 0.5, 0.8, and 1 is shown in Figure 3. All degrees of ionization show a coil-like decrease with N at this concentration and we also see a monotonic expansion of the chain as α is increased at any chain length. A similar plot but at ion concentration $c = 0.01$ mol dm^{-3} is shown in Figure 4. Here we see different behavior for chains of low and high degree of ionization—those with $\alpha < 0.3$ behave somewhat like coil-like chains whereas chains with higher degrees of ionization show the characteristic initial increase until the contour length becomes much greater than the screening length.

For an ion concentration $c = 0.1$ mol dm^{-3} we can obtain scaling exponents for $\langle r^2\rangle$ and $\langle s^2\rangle$ of the form

$$\langle r^2\rangle \approx N^{2\nu_1}$$

$$\langle s^2\rangle \approx N^{2\nu_2}$$

(Note that we have changed notation from eq 4.1 and 4.4 of ref 1 so as to conform to the standard notation for the

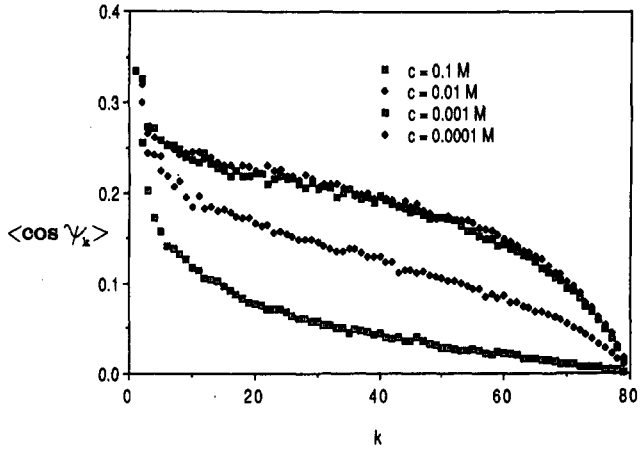

Figure 5. Distribution of bond angles relative to the central bond, plotted as $\langle \cos \psi_k \rangle$, for a chain of 160 beads with a degree of ionization $\alpha = 0.2$ for various salt concentrations.

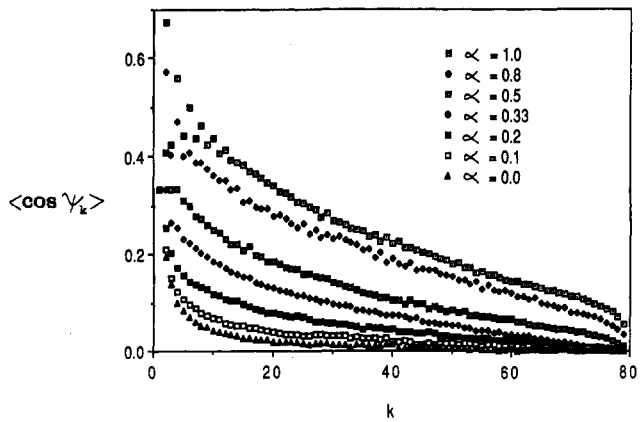

Figure 6. As for Figure 5, but with salt concentration $c = 0.1$ mol dm^{-3} for various degrees of ionization.

exponents ν.) As discussed in ref 1, these exponents should perhaps be viewed more as summaries of the data since it is clear from the data that short chains ($N < 80$) do not exhibit the behavior embodied in the asymptotic scaling regime. For this reason, we only used data for chain lengths greater than 80 beads in obtaining the exponents. In all cases fits were very good. The behavior of $\langle r^2 \rangle$ gave virtually the same exponent ($\nu_1 \cong 0.7$) over the range $\alpha = 1.0$ to $\alpha = 0.1$. Only for uncharged chains does the exponent change ($\nu_1 = 0.6$). By contrast, the behavior of $\langle s^2 \rangle$ showed a more gradual change with decreasing ionization with ν_2 staying at the fully ionized value of 0.78 for $\alpha \geq 0.5$, slowly decreasing to $\nu_2 = 0.7$ at $\alpha = 0.1$, and again $\nu_2 = 0.6$ for uncharged chains. At the lowest degree of ionization, the contour length between charges is about 2 screening lengths and it appears that the scaling behavior of $\langle r^2 \rangle$ does not approach that of uncharged chains until the mean separation between charged beads is larger than a few screening lengths.

The fact that the exponent for $\langle s^2 \rangle$ rises above that for $\langle r^2 \rangle$ as α increases above 0.1 indicates that the mean-square radius of gyration, which depends on the positions of all beads, is influenced more by the electrostatic interactions. Naturally, as $N \to \infty$ this cannot remain true—the true exponents (if they exist) must be equal in this limit. Our results really fall in the intermediate-length regime and reflect the changing average shape of the chain as α and c are varied.[3]

In Figures 5 and 6 we show the distribution of angles $\langle \cos \psi_k \rangle$, where the average of the cosines of the angles between the central bond and the bonds k steps away from the central bond. The values of $\langle \cos \psi_k \rangle$ for $\alpha = 0.2$ and a chain length of 160 beads are shown in Figure 5 for $c = 10^{-1}$, 10^{-2}, 10^{-3}, and 10^{-4} mol dm^{-3}.

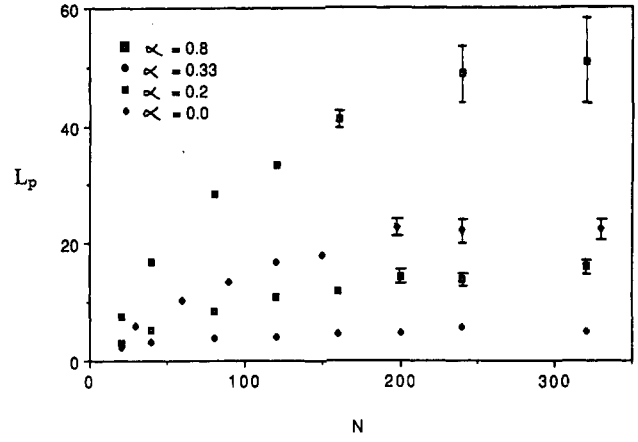

Figure 7. Persistence length L_p as function of chain length for salt concentration $c = 0.1$ mol cm^{-3} and various degree of ionization. Error bars are shown where these are larger than the plotting symbols.

In comparing these results with a similar plot for fully ionized chains,[1] we see that the chains are clearly less stiff, and for $c = 0.1$ mol dm^{-3}, $\langle \cos \psi_k \rangle$ has virtually decayed to zero by $k = 80$; i.e. the infinite-chain persistence length can be obtained directly. For lower concentrations an extrapolation procedure as described in ref 1 would still be required at this low degree of ionization. As before, there is very little difference seen in the graphs for 10^{-3} and 10^{-4} mol dm^{-3}—in both cases the screening lengths (100 Å and 300 Å, respectively) are comparable to the contour length of the chain (≈320 Å).

In Figure 6 we plot $\langle \cos \psi_k \rangle$ for $c = 0.1$ mol dm^{-3} and $N = 160$ for all values of α—the dependence on ionization is rather unexciting, but it is clear that to extract persistence lengths from these results for $\alpha > 0.33$ requires the extrapolation procedure mentioned above.

For the lower degrees of ionization and $c = 0.1$ mol dm^{-3}, the infinite chain persistence length can be calculated directly, in that the persistence length

$$L_p = l \sum_{k=0}^{(N/2)-1} \langle \cos \psi_k \rangle$$

becomes independent of N for $N \geq 200$ beads, i.e. within reachable values of N. This can be seen from Figure 7, where the persistence lengths, L_p, for $c = 0.1$ mol dm^{-3} are shown for $\alpha = 0.8$, 0.33, 0.2, and 0. Although the errors are sometimes large, it is clear that L_p has reached a steady value for $\alpha = 0.2$ and 0.33, but it is still increasingly for $\alpha = 0.8$. At the higher degrees of ionization at $c = 0.1$ mol dm^{-3} and at all degrees of ionization for $c \leq 10^{-2}$ mol dm^{-3}, the infinite chain result cannot be found directly. At $c = 0.1$ mol dm^{-3}, however, there is clear evidence of a flattening of L_p versus N and the extrapolation procedure of ref 1 can be used—viz., the first 15 values of $\langle \cos \psi_k \rangle$ are summed explicitly, the last 20 values are ignored, and the remaining values are fitted to an exponential $\langle \cos \psi_k \rangle \approx e^{-ak}$. These exponential fits are often very good (see, for example, Figure 8), and the resulting fitted values then provide the rest of the terms in the infinite-chain persistence length.

In Table I we have simply collected the various estimates of L_p^∞ for $c = 0.1$ mol dm^{-3}, either directly from Figure 7 or through the extrapolation of $\langle \cos \psi_k \rangle$ for $N = 160$ beads or the actual value of L_p for $N = 320$ beads. The table shows good agreement between these various estimates.

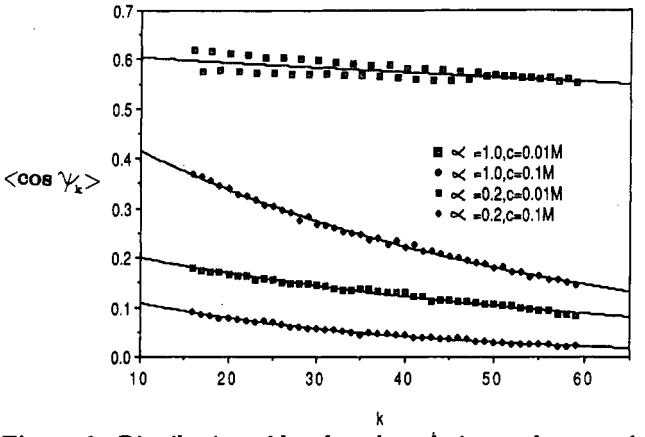

Figure 8. Distribution of bond angles relative to the central bond for a variety of salt concentrations and degrees of ionization together with the corresponding fits to exponential decay, as required for the extrapolation to infinite chain length.

Table I
Various Estimates of the Infinite-Chain Persistence Length for c = 0.1 mol dm^{-3} [a]

	L_p^∞				L_p^∞		
α	extrapolated	direct	L_p, N = 320	α	extrapolated	direct	L_p, N = 320
1.0	61.9		59.9	0.2	12.8	15	16.2
0.8	51.7		50.8	0.1	7.5	9	9.5
0.5	29.9		35.2	0	4.6	5	5.1
0.33	20.4	22	22.5				

[a] The extrapolated L_p^∞ is obtained by fitting $\langle\cos\psi_k\rangle$ to an exponential curve for N = 160 as described in ref 1. The direct L_p^∞ is the steady value attained by L_p for $N \geq 200$.

It is also apparent that L_p^∞ increases only slightly faster than linearly with α, as opposed to the α^2 dependence of the zeroth order theory of Odijk[7] and Skolnick and Fixman.[9] One possible source of such a discrepancy is that we are calculating the persistence length solely as a conformational quantity whereas in refs 7 and 9 it is derived from the energetics of a gently curving space curve. It is shown in ref 10 that the two definitions of persistence length are equivalent in the wormlike limit $N \to \infty$, $l \to 0$, $\theta \to \pi$ such that $1/(1 + \cos\theta)$ and N and l remain finite. Our calculations are not done in this limit but for finite N, l, and θ, and so the two methods of calculating the persistence length are not precisely equivalent for the present model.

Our results for L_p^∞, as obtained by extrapolation, are collected in Table II. The results for $c = 10^{-3}$ and 10^{-4} mol dm^{-3} are somewhat less reliable since the part of the chain that has been fit to an exponential represents only a small part of the decay of $\langle\cos\psi_k\rangle$ for these very stiff chains.

Table II
Extrapolated Values of the Infinite-Chain Persistence Length for Various Values of Degree of Ionization and Ion Concentration[a]

α	10^{-1} mol dm^{-3}	10^{-2} mol dm^{-3}	10^{-3} mol dm^{-3}	10^{-4} mol dm^{-3}
1.0	61.9	290	900	2000
0.8	51.7	270	700	1400
0.5	29.9	115	330	500
0.33	20.4	65	160	150
0.2	12.8	37	72	76
0.1	7.5	14.4	19	23

[a] Results for the lower ion concentrations, where the estimated persistence length greatly exceeds the contour length of the 160-bead chain (used in the extrapolation), are less reliable than the results for $c \geq 10^{-2}$ mol dm^{-3}.

To close this paper, we mention the comparison between our results for L_p^∞ and those, incorporating ionic degrees of freedom through the Poisson–Boltzmann equation, of Le Bret[11] and Fixman.[12] Our previous comparison in ref 1 was rather unfair in that we compared their results for a slightly curved rod of radius 10 Å with our simulation results. However our chain more closely resembles (in the all-trans configuration) a rod of radius 2 Å. On converting the results in ref 12 to represent a rod of radius 2 Å, we find that the predicted persistence lengths are always much smaller than our results, in agreement with intuition. This resolves the "puzzling result" mentioned in ref 1.

References and Notes

(1) Carnie, S. L.; Christos, G. A.; Creamer, T. P. *J. Chem. Phys.* **1988**, *89*, 6484.
(2) Creamer, T. P. Ph.D. Dissertation, University of Western Australia, 1991.
(3) Christos, G. A.; Carnie, S. L. *J. Chem. Phys.* **1989**, *91*, 439.
(4) Kowblansky, M.; Zema, P. *Macromolecules* **1981**, *14*, 166.
(5) Klein, J. W.; Ware, B. R. *J. Chem. Phys.* **1984**, *80*, 1334.
(6) Mills, P.; Anderson, C. F.; Record, M. T., Jr. *J. Phys. Chem.* **1985**, *89*, 3984.
(7) Odijk, T. *J. Polym. Sci. Polym. Phys.* **1977**, *15*, 477.
(8) Miklavic, S. J.; Chan, D. Y. C.; White, L. R. *Colloid Polym. Sci.* **1990**, *268*, 290.
(9) Skolnick, J.; Fixman, M. *Macromolecules* **1977**, *10*, 944.
(10) Yamakawa, H. *Modern Theory of Polymer Solutions*; Harper & Row: New York, 1971; pp 52–55.
(11) Le Bret, M. *J. Chem. Phys.* **1982**, *76*, 6243.
(12) Fixman, J. *J. Chem. Phys.* **1982**, *76*, 6346.

Registry No. PAA (homopolymer), 9003-01-4.